Study on Knock-on Tail Formation in Deuteron Velocity Distribution Function Due to ICRF-Heated Energetic Proton by Using Neutron Diagnostics in the Large Helical Device*)

Daisuke UMEZAKI, Hideaki MATSUURA, Kento KIMURA, Takahito FUKUDA, Kunihiro OGAWA[1,2)], Mitsutaka ISOBE[1,2)], Shuji KAMIO[3)], Yasuko KAWAMOTO[1)] and Tetsutaro OISHI[1,2)]

Department of Applied Quantum Physics and Nuclear Engineering, Kyushu University, Fukuoka 819-0395, Japan
[1)]*National Institute for Fusion Science, National Institutes of Natural Sciences, Toki 509-5292, Japan*
[2)]*The Graduate University for Advanced Studies, SOKENDAI, Toki 509-5292, Japan*
[3)]*Department of Physics and Astronomy, University of California, Irvine, CA 92697, USA*

(Received 9 January 2023 / Accepted 16 May 2023)

In fusion plasmas, energetic ions play a crucial role in plasma heating. Nuclear elastic scattering (NES) is a non-Coulombic scattering process that affects the energy transport between energetic and bulk ions. In the Large Helical Device (LHD), energetic protons produced by neutral beam injection (180 keV) formed a knock-on tail (KT) in deuterons via NES, and the DD neutron emission rate increased by one order of magnitude in relatively high-electron-temperature plasmas. Furthermore, the effect of NES among ion cyclotron range of frequency (ICRF) tail protons and bulk deuterons was investigated at high-electron-temperature plasmas in the LHD. It was found that DD neutron emission rate was increased by a factor of 2 to 4. Changes in ion temperature and plasma density cannot be the only reasons for the increase in DD neutron emission rate. The increment in DD neutron emission rate was reproduced by the Fokker-Planck simulation using the Boltzmann collision integral for NES by assuming the ICRF-tail protons having a high-temperature Maxwellian.

Keywords: nuclear elastic scattering, NES effect, LHD, knock-on tail, ICRF heating

DOI: 10.1585/pfr.18.2402056

1. Introduction

In fusion plasmas, energetic ions play a crucial role in plasma heating. Nuclear elastic scattering (NES) [1, 2] is a scattering process between ions with high relative energy. In NES, a relatively large fraction of energy is transferred in a single scattering event in contrast to Coulomb scattering. Energetic ions produced through nuclear reactions, neutral beam (NB) injection, and others contribute to a formation of a knock-on tail (KT) in an ion velocity distribution function via NES. In an experiment of Joint European Torus (JET), a non-Gaussian energetic component in the D-T neutron emission spectrum was observed [3]. In another JET experiment [4], a KT was measured using a neutral particle analyzer (NPA). The beam protons formed the KT in deuteron velocity distribution function, which resulted in a one order of magnitude increase in the neutron emission rate of high-electron-temperature (8 - 10 keV) plasmas in the Large Helical Device (LHD) [5, 6]. The NES induced enhancement in the slowing-down time of beam deuterons in the LHD [7]. In another JET experiment, energetic deuterium flux was observed using an NPA in the ^{3}He-minority heating deuterium plasma [8]. The NES between bulk deuterons and ion cyclotron range of frequency (ICRF)-tail ^{3}He ions was discussed in Ref. [8]; however, the measured suprathermal tail of deuterium is an order of magnitude larger than that given by the simulation. The reason for this discrepancy has not been clarified yet. The effect of deuterons KT formed by the NES with ICRF-tail ^{3}He ions on the neutron emission spectrum was also investigated by numerical simulation [9].

In the LHD, the ICRF heating systems have been developed [10, 11]. The energy of beam ions is up to 180 keV and the energy of ICRF-tail protons can reach MeV range [12]. In the previous ICRF heating deuterium plasma experiment with a second harmonic scenario performed on the LHD [13], an extra increase in neutron emission rate over the change in ion temperature has not been observed. A KT might not have been formed, because the central electron temperature was not sufficiently increased, i.e., $T_e(0) \sim 5$ keV. As discussed in Ref. [6], an apparent increase in neutron emission rate due to the formation of a KT requires a high-central-electron-temperature ~8 - 10 keV. Hence, it is necessary to perform experiments of high-electron-temperature plasmas to observe an increase in neutron emission rate due to a KT.

author's e-mail: umezaki.daisuke.786@s.kyushu-u.ac.jp
*) This article is based on the presentation at the 31st International Toki Conference on Plasma and Fusion Research (ITC31).

In this research, we attempted to observe the KT effect on the D-D neutron emission rate by ICRF-tail protons in high-electron-temperature LHD plasmas. The ICRF-tail proton spectrum was estimated using a single crystal diamond neutral particle analyzer (DNPA) [14]. The time evolution of neutral emission rate was reproduced through Fokker-Planck (FP) simulation with the Boltzmann collision integral term for the NES. We also compared the FP simulation results with Stix's theoretical model. Furthermore, an ICRF tail in a deuteron velocity distribution function might have been created by second harmonic heating. Hence it is necessary to validate that any increase in the neutron emission rate is indeed due to the KT by checking the absorption power of the second harmonic heating. We report the experimental and simulated results in this paper.

2. Experimental Apparatus

Figure 1 shows a schematic of NBs in LHD experiments reported in this paper. In the experiments, deuterium plasmas were initiated by electron cyclotron resonance heating (ECH). Negative-ion-source-based high-purity hydrogen beam NB#1 was tangentially injected into the deuterium plasma. The beam energy and port through power of NB#1 were approximately 180 keV and 3.5 MW, respectively. The deuteron ratio in NB#1 was suppressed to be less than 1 ppm. Positive-ion-source-based deuterium beam NB#5 was perpendicularly injected. The beam energy and port through power of NB#5 were about 50 keV and 4.5 MW, respectively. NBs #2, #3, and #4 were not used. Two pairs of ICRF antennas were utilized. They are the HAS antenna [15] and the FAIT antenna [16]. The ICRF heating frequency was 38.47 MHz. Other details were the same as in Ref. [12]. The neutron emission rate was measured by ^{235}U fission chambers (FC) and ^{10}B

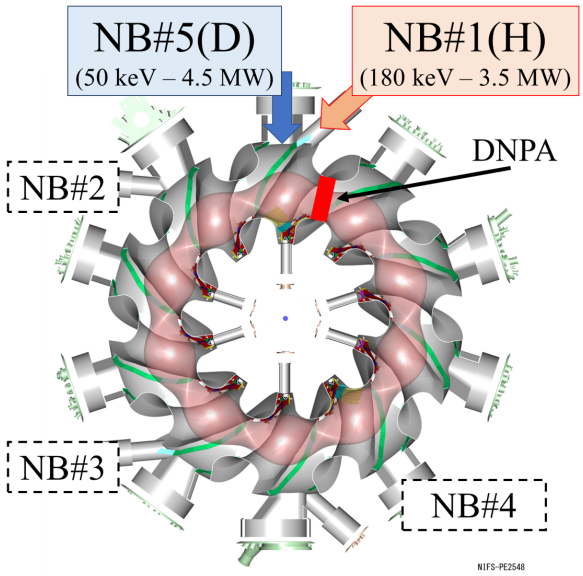

Fig. 1 Schematic view of the NBs and the location of DNPA around the LHD.

counters of the neutron flux monitor [17]. In the experiments, the preset magnetic axis position R_{ax} was 3.60 m, and the toroidal magnetic field strength B_T was 2.75 T with counterclockwise direction from the top view.

In the FP simulation [18], a uniform deuteron plasma accompanied by the deuterium and hydrogen NBs was assumed. As the background Maxwellian plasmas, deuterons, protons, and electrons were considered. In this study, the KT formed in the deuteron velocity distribution function via the NES between bulk deuterons and ICRF-tail protons. To assess the effect of NES on the DD neutron emission rate, we solved the deuteron velocity distribution function through FP simulation including the Boltzmann collision integral term [6, 18–20]. The background particle's density and temperature were given in reference to experimental values at $r/a = 1/2$ (a is averaged LHD plasma minor radius). However, only the electron density n_e was measured, and the experimental deuteron density n_D was unknown. By assuming $n_D = X \times n_e$ and calculating the DD neutron emission rate with consideration of plasma profiles in the LHD, the neutron emission rate can be reproduced when $X = 0.4$ - 0.5. Therefore, in this study, we assumed $n_D = 0.5 \times n_e$ for simplicity. The NES cross section can be assumed an isotropic scattering in the center of mass system [21]. In this study, the ICRF-tail protons velocity distribution function was assumed as an isotropic Maxwellian of an effective temperature T_p^{eff}. T_p^{eff} was changed as a parameter to reproduce the increase in experimental neutron emission rate. The density of ICRF-tail protons was determined with reference to the experimental DNPA data discussed in Sec. 3.2.

In several studies, proton density was estimated using experimental H_α and D_α spectroscopic measurement data $D_\alpha/(D_\alpha + H_\alpha)$ [13]. In this study, the ICRF-tail proton velocity distribution function was assumed by two methods. 1) First, the ICRF-tail proton velocity distribution function was assumed as a Maxwellian of effective temperature T_p^{eff}, and its spectrum was estimated using the DNPA. 2) Second, the ICRF-tail protons density was estimated using $D_\alpha/(D_\alpha + H_\alpha)$ data, and its temperature was determined from Stix's theory [22] as described below. The results of these method were compared. The Stix's theoretical temperature T_p^{theo} is written as follows [12, 22]:

$$T_p^{theo} = \frac{p_{abs}\tau_s}{2n_p}, \tag{1}$$

where p_{abs} is the ICRF absorption power density, $\tau_s = 6.28 \times 10^8 T_e^{3/2}\,[\mathrm{eV}]/(n_e\,[\mathrm{cm}^{-3}] \times \ln\Lambda)$ is the Spitzer slowing-down time, and n_p is proton density. The results of the first and second methods are described in Sections 3.2 and 3.3, respectively.

3. Result and Discussion

3.1 Experimental results

Figure 2 shows the typical waveforms of a deuterium plasma discharge, i.e., #172058, including the time evolu-

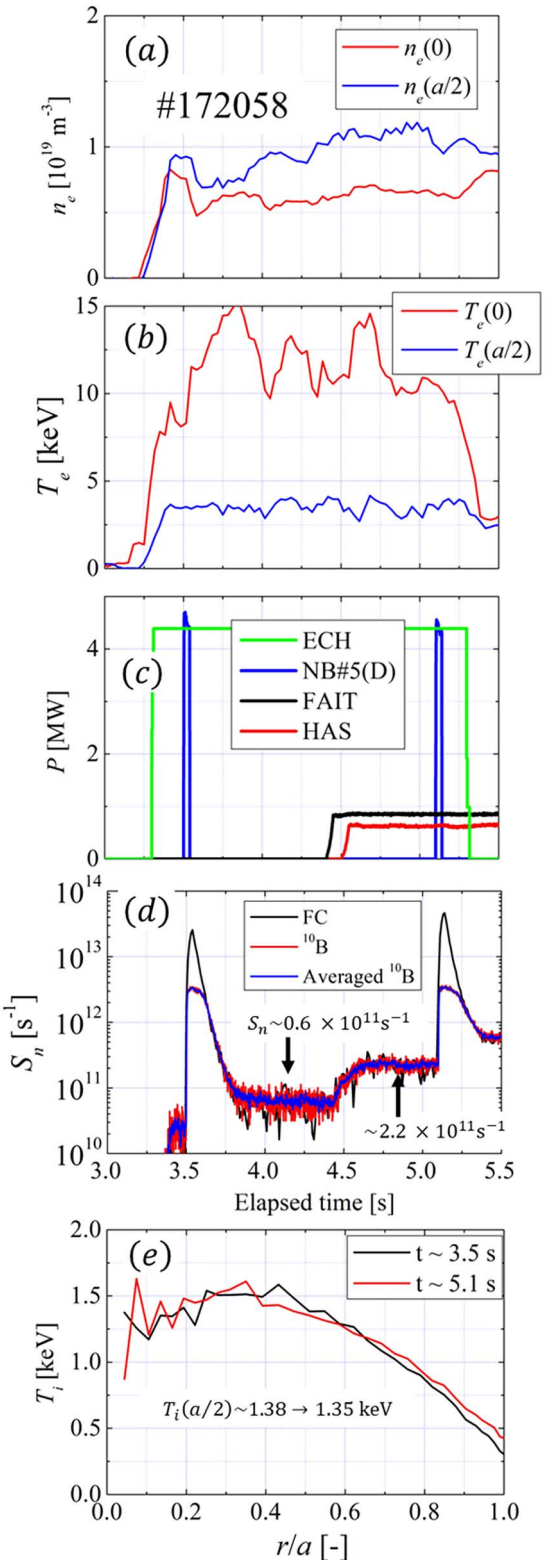

Fig. 2 Time evolutions of deuteron plasma discharge (shot no. #172058). (a) Electron densities at $r = 0$ and $r = a/2$; (b) electron temperatures at $r = 0$ and $r = a/2$; (c) NB#5, ECH and ICRF injection power; (d) neutron emission rate; (e) ion temperature profiles at $t \sim 3.5$ and $t \sim 5.1$ s.

tion of, (a) electron density at radii $r = 0, a/2$, (b) electron temperature at radii $r = 0, a/2$, (c) NB#5(D), ECH and ICRF injection power, (d) neutral emission rate, and (e) ion

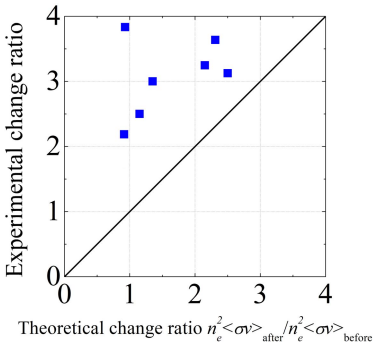

Fig. 3 Relationship between the change ratio of the neutron emission rate before and after the ICRF heating, and the change ratio of the neutron emission rate calculated from the experimental ion temperature and electron density before and after the ICRF heating.

temperature profiles at $t \sim 3.5, 5.1$ s. Deuteron plasma was initiated at 3.3 s. The ion temperature was measured by the charge exchange recombination spectroscopy at 3.5 (5.1) s before (after) the ICRF heating and after steady-state attainment of neutron emission rate. To clearly observe an increase in the neutron emission rate due to the formation of KT, the ICRF heating was started at 4.5 s after the decay of the neutron emission rate caused by NB#5(D). In several discharges (such as Fig. 2), the neutron emission rate increased in spite of the decrease or slight change in ion temperature. In addition, the central electron temperature was ~10 keV which is significantly higher than in the previous experiments [13].

In Fig. 3, the change ratio of the neutron emission rate before and after the ICRF heating, $S_n^{\rm after}/S_n^{\rm before}$, is plotted on the vertical axis, while the change ratio of the neutron emission rate calculated from the experimentally obtained ion temperature and electron density before and after the ICRF heating, $n_e^2\langle\sigma v\rangle_{\rm after}/n_e^2\langle\sigma v\rangle_{\rm before}$, is displayed on the horizontal axis. The electron density n_e and ion temperature used in the calculation are the experimental values at $r = a/2$. The deuteron density is assumed to be equal to n_e, and $\langle\sigma v\rangle$ is calculated from the measured ion temperature. The shots shown in Fig. 3 are ion temperatures that did not change significantly before and after ICRF injection. After ICRF heating, the experimental neutron emission rate increased by a factor of 2 - 4, and the increment was larger than that of the change ratio calculated from the experimental ion temperature and plasma density. The ICRF-tail protons knocked the bulk deuteron, and KT might have been formed in the deuteron velocity distribution function.

3.2 Measurement of ICRF-tail energetic protons by DNPA

The number of ICRF-tail protons was estimated with a DNPA. Figure 4 shows the lines of sight of DNPA channels 1 and 7. As the energetic protons heated by the ICRF wave were trapped in the helical ripple, channels 1 and 7,

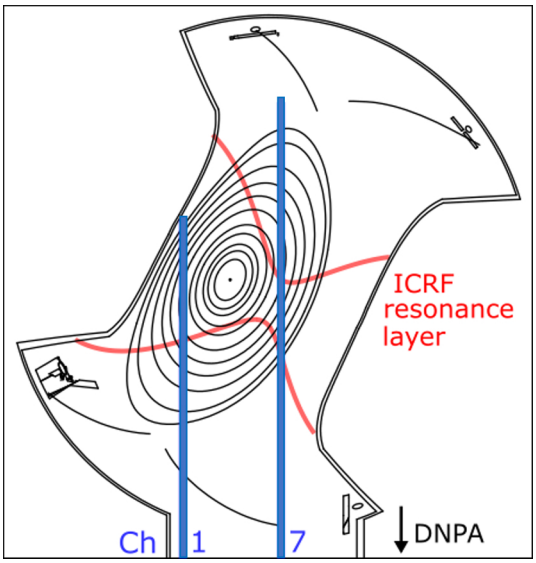

Fig. 4 Lines of sight of DNPA channels 1 and 7.

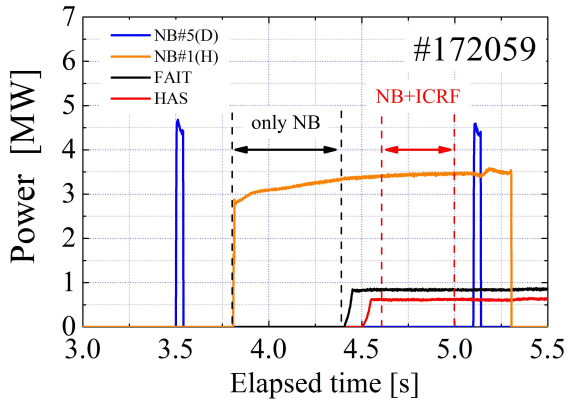

Fig. 5 Typical waveform of the shot #172059 for DNPA measurement.

which measured the bottom and upper helical ripples, respectively. In this study, only the signals from channel 1 is utilized. Additionally, the effect of neutron on DNPA counts can be ignored [23] in this experiment. To ensure sufficient NPA counts, we needed a neutral particle supply, such as an NB, for a charge exchange with ions. In this study, we compared two types of NPA counts: 1) the integrated counts of DNPA during NB#1(H) only, 2) the integrated counts of DNPA during NB#1(H) and ICRF heating. Figure 5 shows the typical waveform of shot #172059 for DNPA measurement. In #172059, NB#1(H) was injected after 3.8 s, and the ICRF wave was injected after 4.5 s. The DNPA counts at 3.8 - 4.3 (4.6 - 5.0) s were integrated as the only time zone for NB#1(H) (NB#1(H) + ICRF heating). The same data integration was performed in other similar shots to improve the DNPA measurement accuracy.

We estimated the number of ICRF-tail protons by subtracting type-1 from type-2 data. Figure 6 shows the DNPA

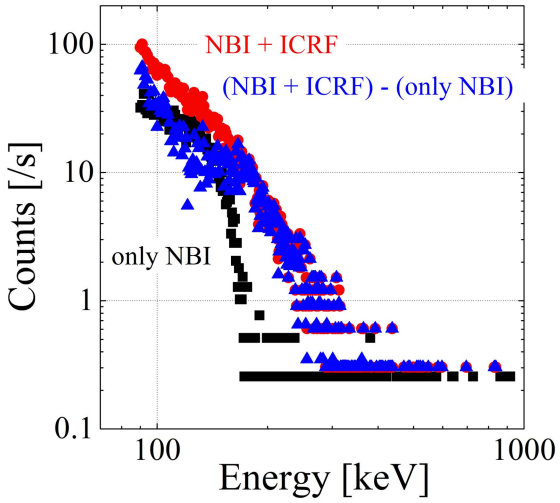

Fig. 6 DNPA count rates of NB + ICRF heating (red points); only NB (black points) and the data produced by subtraction of only NB from NB + ICRF heating (blue points).

integrated counting rates of type-1, type-2, and subtracted data. Within 90 - 180 keV, ICRF-tail protons might have been present in almost the same amount as NB#1(H). Over 180 keV, ICRF-tail protons might have been present considerably more than the NB#1(H) alone. The calculated NB#1(H) absorption power was approximately 1.8 MW.

3.3 FP and Boltzmann collision integral simulation

The ICRF-tail proton velocity distribution function for the Boltzmann collision integral was assumed as the Maxwellian of temperature T_p^{eff}, which intersected the NB#1(H)'s velocity distribution function with reference to the DNPA data. The NB#1(H)'s velocity distribution function was calculated by the DELTA5D code [24], in the same manner as that in Ref. [25], and its absorption power was 1.8 MW. The time evolution of deuteron velocity distribution function was calculated via the FP simulation with the Boltzmann collision integral using the assumed ICRF-tail proton velocity distribution function. Moreover, the time evolution of the neutron emission rate was also calculated. To reproduce the experimental time evolution of the neutron emission rate, the proton's temperature T_p^{eff} was changed as a parameter. Here we focused on #172058 as a typical example to reproduce the neutron emission rate. Figure 7 shows the simulated and experimental time evolutions of the neutron emission rate. The neutron emission rate was normalized at the ICRF heating injected time of 4.4 s. When T_p^{eff} = 50 keV, time evolution of the neutron emission rate was reproduced. Figure 8 show the deuteron, assumed ICRF-tail proton, and NB#1(H)'s proton velocity distribution functions. The temperature T_p^{eff} = 50 keV obtained by the FP simulation was smaller than the effective ICRF-tail temperatures (70 - 250 keV) measured by NPAs in other LHD experiments [26]. As a possible explanation,

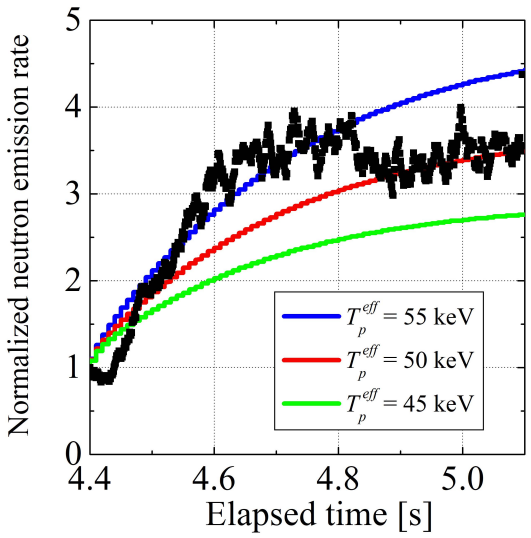

Fig. 7 Time evolution of experimental (black dots) and simulated neutron emission calculated by assuming T_p^{eff} = 45 (green line), 50 (red line), 55 (blue line) keV.

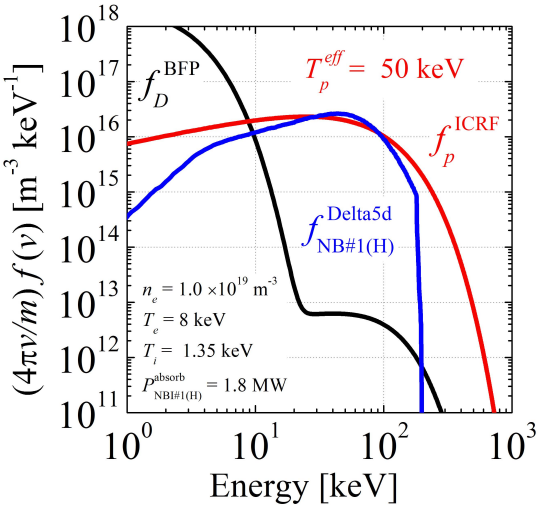

Fig. 8 Deuteron velocity distribution function (black line) calculated via the FP simulation, the assumed ICRF-tail proton velocity distribution function (red line), and NB#1(H)'s velocity distribution function calculated via the Delta5d code.

our FP simulation assumed uniform plasmas. However, the ICRF-tail ion velocity distribution function generally has an anisotropy in a heating direction, and the KT may exhibit anisotropy in the same direction. The assumption of a uniform plasma was expected to be a cause of overestimation of the KT and neutron emission rate increment, which can lead to underestimation of the ICRF-tail proton's temperature in this simulation. Furthermore, as described in section 2, we assumed n_D/n_e as 0.5 for the FP simulation. If the plasma contains many impurities, the actual n_D/n_e may be smaller than 0.5. In such low n_D/n_e plasmas, it is expected that T_p^{eff} should be higher than 50 keV

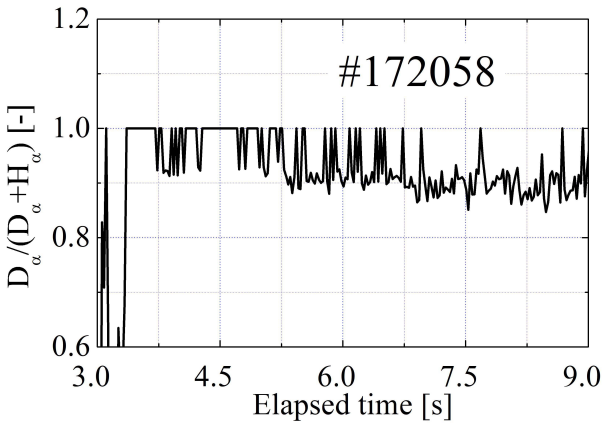

Fig. 9 Time evolution of $D_\alpha/(D_\alpha + H_\alpha)$.

in order to reproduce the observed increase in experimental neutron emission rate. This is consistent with the experimental effective temperature that has been measured by an NPA in previous studies [26]. The density calculated from the assumed ICRF-tail proton velocity distribution function was 2.38×10^{18} m^{-3}, which was larger than the density estimated by $D_\alpha/(D_\alpha + H_\alpha)$ data, and it is approximately $n_p = 6/25 \times n_e$.

3.4 Estimation of theoretical ICRF-tail ion temperature

To calculate the theoretical ICRF-tail ion temperature using Eq. (1), we estimated the proton density using the $D_\alpha/(D_\alpha + H_\alpha)$ data. Figure 9 shows the time evolution of $D_\alpha/(D_\alpha + H_\alpha)$ in #172058. The ratio changed to around 90%, and thus, the proton density was estimated as $n_p = n_D/9 = n_e/18$. The ICRF absorption power p_{abs} was assumed 75% with reference to Ref. [13] and [26]. The theoretical ICRF-tail proton temperature T_p^{theo} was approximately 1.2 MeV using the above discussed values. If the similar calculation of Sec. 3.2 was performed with the proton Maxwellian, which has $n_p = n_e/18$ and T_p^{theo} = 1.2 MeV, the increase in neutron emission rate was approximately 500 times, and the experimental increment cannot be reproduced because the simplified theory ignores ion loss and overestimates the number of energetic ions.

The deuteron 2nd harmonic heating absorption power was also calculated through the same way in Ref. [26]. The deuteron 2nd absorption power was less than 5% in this experimental condition.

4. Conclusions

The effect of NES between ICRF-tail protons and bulk deuterons on the D-D neutron emission rate in the LHD was investigated. In the several high-electron-temperature plasmas, the increase in neutron emission rate by a factor of 2 to 4 was observed after the ICRF proton heating, which cannot be explained by changes in ion temperature and plasma density alone. The KT in the deuteron ve-

locity distribution function may be formed via the NES with the ICRF-tail energetic protons. Moreover, the number of ICRF-tail protons was estimated using the DNPA. Within 90 - 180 keV, the ICRF-tail protons might have been present in almost the same amount as NB#1(H). In over 180 keV, the ICRF-tail protons might have been present considerably more than NB#1(H). The FP simulation using the Boltzmann collision integral for the NES was performed, and the time evolution of deuteron velocity distribution function was solved. The ICRF-tail protons velocity distribution function was assumed as a Maxwellian of temperature T_p^{eff} with reference to the DNPA counts, and the experimental neutron emission rate was reproduced by $T_p^{eff} = 50$ keV. By this method, using the NES effect on the neutron emission rate, ICRF-tail proton velocity distribution function can be possibly estimated. Furthermore, Stix's theoretical temperature was calculated by inferring the proton density from the $D_\alpha/(D_\alpha + H_\alpha)$ measurements. However, the FP simulation was not able to reproduce the experimental neutron emission rate using Stix's theoretical temperature and the proton density estimated by $D_\alpha/(D_\alpha + H_\alpha)$. This was because the simplified theory ignores particle loss and overestimates the number of energetic ions.

Future works should be aimed at validating the formation of KT by ICRF-tail energetic particles and the increase in neutron emission rate in high-ion-temperature ($T_i > 2$ keV) plasmas, where the neutron emission rate hardly changes with the ion temperature.

Acknowledgment

This work was supported by JST SPRING, Grant Number JPMJSP2136. The authors would like to thank Dr. K. Saito for discussing the ICRF absorption power and Dr. D.A. Spong for allowing them to use his code.

Data availability statement

The LHD data can be accessed from the LHD data repository at https://www-lhd.nifs.ac.jp/pub/Repository_en.html.

[1] J.J. Devany and M.L. Stein, Nucl. Sci. Eng. **46**, 323 (1971).
[2] S.T. Perkins and D.E. Cullen, Nucl. Sci. Eng. **77**, 20 (1981).
[3] J. Källne *et al.*, Phys. Rev. Lett. **85**, 3358 (1997).
[4] A.A. Korotkov *et al.*, Phys. Plasmas **7**, 957 (2000).
[5] H. Matsuura *et al.*, Nucl. Fusion **61**, 094001 (2021).
[6] H. Matsuura *et al.*, Phys. Plasmas **29**, 092502 (2022).
[7] H. Matsuura *et al.*, Nucl. Fusion **60**, 066007 (2020).
[8] F.S. Zaitsev *et al.*, Plasma Phys. Control. Fusion **49**, 1747 (2007).
[9] M. Nocente *et al.*, Nucl. Fusion **53**, 053010 (2013).
[10] T. Mutoh *et al.*, Phys. Rev. Lett. **85**, 4530 (2000).
[11] R. Kumazawa *et al.*, Plasma Phys. Control. Fusion **45**, 1037 (2003).
[12] K. Saito *et al.*, Fusion Sci. Technol. **58**, 515 (2010).
[13] R. Seki *et al.*, Plasma Fusion Res. **15**, 1202088 (2020).
[14] S. Kamio *et al.*, J. Inst. **14**, C08002 (2019).
[15] H. Kasahara *et al.*, 38th EPS Conf. Plasma Physics **35**, 897 (2011).
[16] K. Saito *et al.*, Fusion Eng. Des. **96-7**, 583 (2015).
[17] M. Isobe *et al.*, IEEE Trans. Plasma Sci. **46**, 2050 (2018).
[18] M.M. Rosenbluth *et al.*, Phys. Rev. **107**, 1 (1957).
[19] H. Matsuura and Y. Nakao, Phys. Plasmas **13**, 062507 (2006).
[20] M. Nakamura *et al.*, J. Phys. Soc. Jpn. **75**, 024801 (2006).
[21] D.E. Cullen and S.T. Perkins, Nucl. Sci. Eng. **81**, 75 (1982).
[22] T.H. Stix *et al.*, Nucl. Fusion **15**, 737 (1975).
[23] S. Kamio *et al.*, Rev. Sci. Instrum. **91**, 113304 (2020).
[24] D.A. Spong, Phys. Plasmas **18**, 056109 (2011).
[25] S. Sugiyama *et al.*, Plasma Phys. Control. Fusion **60**, 105003 (2018).
[26] S. Kamio *et al.*, Nucl. Fusion **62**, 016004 (2022).